**Biogeosciences
Discussions**

Twentieth century δ^{13}C variability in surface water dissolved inorganic carbon recorded by coralline algae in the northern North Pacific Ocean and the Bering Sea

B. Williams[1], J. Halfar[1], R. S. Steneck[2], U. G. Wortmann[3], S. Hetzinger[1,*],
W. Adey[4], P. Lebednik[5], and M. Joachimski[6]

[1]Department of Chemical and Physical Sciences, University of Toronto,
Mississauga, Ontario, Canada
[2]Darling Marine Center, University of Maine, Walpole, Maine, USA
[3]Department of Geology, University of Toronto, Mississauga, Ontario, Canada
[4]Department of Botany, Smithsonian Institution, Washington, D.C., USA

[5]ARCADIS US Inc., Walnut Creek, California, USA
[6]Institut für Geologie und Mineralogie, Universität Erlangen, Erlangen, Germany
[*]present address: IFM-GEOMAR, Leibniz Institute of Marine Sciences, Kiel, Germany

Correspondence to: B. Williams (branwen.williams@utoronto.ca)

**Twentieth century
δ^{13}C variability in
surface water**

B. Williams et al.

Printer-friendly Version

Interactive Discussion

Title Page

Abstract | Introduction

Conclusions | References

Tables | Figures

|◄ | ►|

◄ | ►

Back | Close

Full Screen / Esc

Printer-friendly Version

Interactive Discussion

Abstract

Oxygen isotopes and Mg/Ca ratios in long-lived coralline algae record ambient seawater temperature in their calcified tissues over time. Similarly, carbon stable isotopes (δ^{13}C) in the calcified tissue may record δ^{13}C values of ambient seawater dissolved inorganic carbon. Here, we measured δ^{13}C in the coralline algae *Clathromorphum nereostratum* to test the feasibility of reconstructing the intrusion of anthropogenic CO_2 into the northern North Pacific Ocean and Bering Sea. δ^{13}C was measured in the high Mg-calcite calcified tissue of three *C. nereostratum* specimens from two islands 500 km apart in the Aleutian archipelago. In the records spanning 1887 to 2003, the average rate of decline in δ^{13}C values increased from 0.03‰ yr^{-1} in the 1960s to 0.1‰ yr^{-1} in the 1990s, which was higher than expected due to solely the δ^{13}C-Suess effect. Deeper water in this region exhibits higher concentrations of CO_2 and low δ^{13}C values. Transport of deeper water into surface water (i.e., upwelling) is increased when the Aleutian Low is intensified. We hypothesize that the acceleration of δ^{13}C decline may result from an increase in upwelling from the 1960s to 1990s, which in turn was driven by an increase in the intensity of the Aleutian Low. Detrended δ^{13}C records also vary on 4–7 years and bidecadal timescales supporting an atmospheric teleconnection of tropical climate patterns to the northern North Pacific Ocean and Bering Sea manifested as changes in upwelling.

1 Introduction

The world's oceans have taken up approximately half of the anthropogenic CO_2 emitted into the atmosphere (Sabine et al., 2004a). Since anthropogenic emissions of CO_2 continue to increase, understanding and constraining CO_2 uptake by the ocean is of considerable importance. The ability of the ocean to take up anthropogenic CO_2 varies widely depending largely on the local/regional water temperature, ocean circulation, and biological productivity. This is particularly true in the subarctic Pacific Ocean,

where estimates of carbon uptake rates from direct measurements and proxy records vary substantially (Newsome et al., 2007; Quay et al., 2003; Tanaka et al., 2003), likely as a result of large seasonal and interannual variability in the physical and biological controls on surface water CO_2 (Sabine et al., 2004b). Therefore, robust, high-resolution records of seawater CO_2 in this region are needed to more accurately constrain the role of the northern North Pacific Ocean and Bering Sea in absorbing anthropogenic CO_2.

The ratio ^{13}C/^{12}C of seawater dissolved inorganic carbon (DIC), expressed as δ^{13}C$_{DIC}$, is a useful method to measure the intrusion of anthropogenic CO_2 into surface waters (Quay et al., 1992). Specifically, δ^{13}C$_{DIC}$ values record the δ^{13}C-Suess effect (i.e., the burning of isotopically "light" fossil fuels, which decreases the δ^{13}C value of carbon reservoirs), and δ^{13}C in atmospheric CO_2 at Pt. Barrow, Alaska decreased 0.02‰ yr^{-1} from the early 1980s to the early 2000s (Keeling et al., 2001). In contrast, repeated cruises in the subarctic Pacific recorded little to no decrease in δ^{13}C values of surface water DIC between 1970 and 1990 (Quay et al., 2003) while δ^{13}C$_{DIC}$ values decreased 0.012‰ yr^{-1} from 1997 to 2001 at the western North Pacific station KNOT (Tanaka et al., 2003). In these studies, the depressed influence of the δ^{13}C-Suess effect in the surface waters of the subarctic Pacific water was attributed to rapid renewal of surface waters which prevents the subpolar gyres from equilibrating with the atmosphere (Quay et al., 2003). This reduces the penetration of atmospheric CO_2 into the surface waters, and drives the disequilibrium between atmospheric CO_2 and surface water δ^{13}C$_{DIC}$ values. However, instrumental δ^{13}C$_{DIC}$ measurements are limited both in temporal (i.e., repeat cruise data limited to two data points) and spatial (i.e., one location at station KNOT) distribution, and the rate of the δ^{13}C decrease recorded in multi-decadal proxy records from different locations in the subarctic Pacific exceeds that of the instrumental records (e.g., 0.02 to 0.06‰ yr^{-1} (Newsome et al., 2007; Schell, 2001)). Although these proxy records are useful to supplement instrumental data, their source from marine mammals has inherent disadvantages. For example, it is difficult to differentiate changes in the baseline δ^{13}C$_{DIC}$ relating to anthropogenic causes from temporal shifts in foraging zones of the marine mammals that

have different isotopic values at the base of the food web (Newsome et al., 2007; Hirons et al., 2001). Variability within a marine mammal sample set, i.e., in size, gender, and age, may also obscure baseline changes (Hobson et al., 2004). In addition to the marine mammal-derived records, δ^{13}C values from a gorgonian soft coral in the

5 Alaskan stream declined at a rate of 0.015‰ yr^{-1} (Williams et al., 2007). Records from these corals are valuable as the corals are stationary throughout their life and thus not subject to migration or shift in foraging zones; however, the available records is limited and the factors that control the δ^{13}C values of particulate organic matter, their primary food source, are still poorly understood. Therefore, a robust source of proxy

10 δ^{13}C$_{DIC}$ reconstructions from which to constrain the subarctic δ^{13}C-Suess effect was not available prior to this study.

Coralline algae are a new climate archive in the subarctic regions (Halfar et al., 2008; Kamenos et al., 2009). In particular, paleo-temperature reconstructions extending to 1887 have been derived from the coralline algae *Clathromorphum nereostratum* (Halfar

15 et al., 2007; Hetzinger et al., 2009), a species which is abundant throughout the Aleutian Islands (Lebednik, 1976). Measurements of skeletal δ^{18}O and Mg/Ca in *C. nereostratum* combined with visible annual growth increments in the calcified tissue have yielded robust growth chronologies with sub-annual resolution (Halfar et al., 2007; Hetzinger et al., 2009). Furthermore, δ^{13}C records from coralline algae theoretically are

20 superior to existing subarctic Pacific δ^{13}C animal-based proxy reconstructions because coralline algal skeletal δ^{13}C values are not confounded by changes in the diet, foraging patterns, food web dynamics. Therefore, the goal of this paper is to demonstrate the potential of utilizing *C. nereostratum* as recorders of seawater δ^{13}C$_{DIC}$ and extract robust, high-resolution records of subarctic δ^{13}C$_{DIC}$.

2 Methods

2.1 Sample collection

Two specimens of the coralline alga *C. nereostratum* (Attu 11-4 and AM4-1) were collected live from 10 m depth during a research cruise in August 2004 from the Aleutian Islands (Fig. 1). Attu 11-4 was collected offshore of the southern side of Attu Island (52°47.79 N, 173°10.80 E) and was primarily influenced by the Alaskan Stream. The Alaskan Stream originates in the Gulf of Alaska and turns into the Bering Sea through the Aleutian Islands passages where it is the dominant source of relatively warm, fresh and nutrient-rich water (Reed and Stabeno, 1994). AM4-1 was collected offshore of the northern side of Amchitka Island (51°42.72 N, 179°23.83 W). The US National Herbarium of the Smithsonian Institution in Washington, D.C. provided a third sample collected live in 1969 from 25 m deep offshore of the northeast side of Amchitka Island (AM-KR-80; 51°41.67 N, 179°28.33 W). Both specimens from offshore Amchitka Island were bathed by the Bering Sea.

2.2 Sample preparation and analyses

Untreated algal specimens AM4-1 and Attu 11-4 were sectioned in half and roughly polished onboard the research cruise. A 3 mm thick slice was removed from the museum specimen AM-KR-80 and mounted onto thin section glass. In the lab, the sections were polished with decreasing grit sizes on a Struers Labopol polishing disk. Polished sections were then photographed using an Olympus reflected light microscope attached to an automated sampling stage-imaging system equipped with geo.TS software (see (Hetzinger et al., 2009) for details). Annual increments in the calcified tissue were clearly visible in the resulting high quality images and were digitally mapped using the geo.TS software. This allowed for the location of each sample milled for stable isotope analysis (see below) to be carefully digitized on the photomosaic (Fig. 2). In addition, the widths of each annual growth increment were measured using the geo.TS software.

Full Screen / Esc

Printer-friendly Version

Interactive Discussion

Polished and photographed sections were cleaned in an ultrasonic bath for three ten-minute intervals with deionized water and dried overnight. Working from the outside edge of the specimen which represents the most recent growth toward the oldest part of the sample, material for stable isotope analyses was removed using a high-precision, computer-driven micromill attached to an x, y, and z stage using digitized milling path positions. Sampling resolution for stable isotope analysis varied from one to twelve samples per growth increment depending on the width of the growth increment. Removed material was analyzed for δ^{13}C (δ^{13}C = ‰ deviation of the ratio of stable carbon isotopes ^{13}C:^{12}C relative to Vienna Peedee Belemnite Limestone Standard; VPDB) and δ^{18}O (δ^{18}O = ‰ deviation of the ratio of stable oxygen isotopes ^{18}O:^{16}O relative to Vienna Peedee Belemnite Limestone Standard (VPDB)). AM4-1 samples were introduced into a Thermo-Finnigan MAT253 gas source isotope ratio monitoring mass spectrometer via a Finnigan Gas Bench in the Geobiology Isotope Laboratory at the University of Toronto. The standard deviation of the mean of duplicate measurements was ±0.16‰ for δ^{13}C and ±0.08‰ for δ^{18}O. At least 10% of all samples were run in duplicate. δ^{13}C and δ^{18}O values of AM-KR-80 and Attu 11-4 were analyzed at Erlangen University, Germany according to Hetzinger et al. (2009).

2.3 Data analyses

The predicted isotopic equilibrium values for δ^{13}C and δ^{18}O in inorganic high-Mg calcite were estimated from the equations of Romanek et al. (1992) and Kim and O'Neil (1997), respectively, with a correction of 0.17‰ for each mol% Mg for predicted δ^{18}O (Jimenez-Lopez et al., 2006). The δ^{13}C value of seawater was calculated from the average of six measurements from less than 15 m depth taken in June and August during two cruises in the northern Pacific during 1992 and 1993 (cruise ID: 31VIC92_0 and 3250210_1; data obtained from http://cdiac.ornl.gov/oceans/home.html; Key et al., 2004). The δ^{18}O value of seawater was calculated from the average of 33 measurements from less than 15 m depth taken in June and August in 1990, 1993, and 1995

(data obtained from http://data.giss.nasa.gov/o18data; Cooper et al., 1997; Munchow et al., 1999; and Schmidt et al., 1999).

Chronologies developed in Halfar et al. (2007) and Hetzinger et al. (2009) (also see Sect. 3.1) were applied to the specimens. Isotope data were interpolated to monthly intervals, and then subsequently resampled to annual resolution using AnalySeries software (Paillard et al., 1996). T-tests compared average δ^{13}C values from 1937 to 1967 for AM-KR-80 and Attu 11-4 and from 1968 to 2003 for AM4-1 and Attu 11-4. Attu 11-4 was combined with AM4-1 from 1967–2003 and the dataset was smoothed using a 7-year running average from 1937–2003. The line of best fit was calculated using SigmaPlot (Systat Software Inc., San Jose, CA) for this dataset to determine decadal rates of decrease from the 1960s to 2003. The specimen-specific offset for AM-KR-80 (see Sect. 3.3) prevented the inclusion of this sample in this dataset. The Aleutian Low Pressure Index (ALPI) is the most important index of climate-ocean dynamics in the North Pacific/Bering Sea (Benson and Trites, 2002; McFarlane et al., 2000). Annually-resolved ALPI data (Beamish et al., 1997; http://www.pac.dfo-mpo.gc.ca/science/species-especes/climatology-ie/cori-irco/indices/alpi.txt) were also smoothed with a 7-year running mean. To create a robust dataset for time series analysis, each of the original annually-resolved algal δ^{13}C records were normalized by subtracting the mean and dividing by the standard deviation. The resulting records were then combined to form a dataset comprised of Attu 11-4 and AM-KR-80 from 1937 to 1967 and Attu 11-4 and AM4-1 from 1968 to 2003. The line of best fit was calculated using SigmaPlot and the resulting residuals were used to produce a detrended δ^{13}C dataset. Wavelet analysis (Torrence and Compo, 1998) using IDL Wavelet Toolkit (available at: http://paos.colorado.edu/research/wavelets/) was applied to the combined and detrended dataset to determine the dominant modes of climate variability.

3   Results

3.1   Growth increments and specimen chronologies

The three specimens displayed clear growth increments in the calcified tissue. The width of the annual growth increment varied from 140 to 680 μm with an average of 381 μm for all three specimens. There was no ontogenic or secular change in annual growth increment widths over time in any of the specimens.

Seasonal variability in Mg/Ca ratios in all of the specimens and δ^{18}O values in Attu 11-4 confirmed the annual periodicity of the growth increments (Halfar et al., 2007; Hetzinger et al., 2009). The outermost growth increment in all of the specimens was formed during the summer of the specimen collection and did not represent a whole year of growth. In specimens AM4-1 and Attu 11-4, the year prior to collection was assigned to the first full skeletal growth increment. In specimen AM-KR-80, the first full year of growth was not sampled and the year two-years prior to collection was assigned to the first full growth increment. Therefore, from Amchitka Island, 35 years were sampled from 1968 to 2003 in specimen AM4-1 and 31 years were sampled from 1937 to 1967 in AM-KR-80. From Attu Island, 116 years were sampled from 1887–2003 in specimen Attu 11-4.

3.2 δ^{13}C and δ^{18}O isotopes

Annually-averaged δ^{13}C and δ^{18}O values ranged from −2.5 to 2.6‰ and −2.2 to −1.0‰, respectively, for all specimens (Fig. 3). δ^{13}C and δ^{18}O values positively correlated in AM4-1 ($r^2 = 0.31$), but did not correlate in Attu 11-4 and AM-KR-80 (Fig. 3). Average δ^{13}C values for Attu 11-4 and AM4-1 were depleted relative to predicted isotopic equilibrium by 3.5 and 3.0‰, respectively, for the period of 1992 and 1993 (Fig. 3). Average δ^{18}O values for the same specimens were depleted relative to predicted isotopic equilibrium by 2.2 and 2.0‰, respectively, for the period of 1990, 1993, and 1995 (Fig. 3). Isotope values for AM-KR-80 were not compared to predicted

isotopic equilibrium as this specimen was collected prior to the early 1990s and before instrumental measurements of seawater isotopes were obtained close to the Aleutian Islands.

3.3 δ^{13}C records

δ^{13}C values in AM4-1 and Attu 11-4 decreased from the mid-1960s to 2003. Since AM-KR-80 did not show a similar decrease, no ontogenetic trend in δ^{13}C values was present with age. Based on the smoothed 3-year running mean of the annually interpolated data, δ^{13}C values in the longest dated record, Attu 11-4, increased from 0.7‰ in 1887 to a maximum of 1.9‰ in 1917 before decreasing to −2.0‰ in 2003 (Fig. 4). δ^{13}C values in AM-KR-80 did not change secularly over the duration of the record (1937–1967), with δ^{13}C values of −0.4‰ at the start and −0.7‰ at the end of the record (Fig. 4). AM-KR-80 was collected prior to the beginning of growth of AM4-1, so direct comparisons between the two records are difficult, however δ^{13}C values at the end of the AM-KR-80 record in 1967 were 0.6‰ lower than at the start of the AM4-1 record in 1968 (Fig. 4). In addition, the δ^{13}C values for AM-KR-80 (average δ^{13}C = −0.5‰) were significantly lower than for Attu 11-4 (average δ^{13}C = 1.2‰) from 1937–1967 (t-test, $p < 0.0001$) while δ^{13}C values in AM4-1 were the same as Attu 11-4 (average δ^{13}C = −0.1 for both) from 1968–2003 (Fig. 5). δ^{13}C values from the best-fit line were relatively constant from the 1940s to the 1960s before a strong overall decrease of 2.5‰ from the 1960s to 2000 (Fig. 6). Decadal rates of decrease were 0.3‰ for the 1960s, 0.5‰ for the 1970s, 0.7‰ for the 1980s and 1.0‰ for the 1990s (Fig. 6). Wavelet analysis of the detrended and combined δ^{13}C dataset documents significant spectral power at 4–7 years during the 1960s and at ~16 years throughout the record (Fig. 7).

4   Discussion

4.1   Carbon and oxygen isotopes

C. nereostratum forms calcite depleted in both δ^{13}C and δ^{18}O relative to predicted iso-
topic equilibrium (Fig. 3). However, since δ^{13}C and δ^{18}O covary in only one specimen
(AM4-1), and the range in δ^{18}O values is small, we hypothesize that the correlation
between δ^{13}C and δ^{18}O values in this specimen largely reflects anthropogenically-
driven changes in the isotopes relating to secular variability in δ^{13}C$_{DIC}$ (δ^{13}C-Suess
effect; see below) and temperature/salinity (warmer/less saline; see Halfar et al., 2007),
rather than a kinetic effect common to all *C. nereostratum*. Depleted δ^{18}O values rela-
tive to predicted equilibrium are consistent with previous studies, and are expected to
be species-specific and constant over time, thus facilitating the use of coralline algal-
derived oxygen isotope archives for paleoceanographic reconstructions (e.g., Halfar et
al., 2000, 2007, 2008; Lee and Carpenter, 2001; Wefer and Berger, 1991). Similar to
δ^{18}O, δ^{13}C values in *C. nereostratum* are also depleted relative to predicted isotopic
equilibrium by 3–3.5‰ (Fig. 3). Metabolic processes such as respiration and photo-
synthesis may alter δ^{13}C values resulting in observations that deviate from predictions
based on isotopic equilibrium (Swart, 1983). Respiration in the calcifying microenvi-
ronment may cause ^{13}C-depletion in CO_2. On the other hand, photosynthesis may
cause ^{13}C-enrichment in the same CO_2 microenvironment within the calcified tissue
(i.e., photosynthesis removes ^{12}C). The δ^{13}C values that we measured were depleted
relative to equilibrium predictions. This result indicates that respiratory CO_2 contributed
a significant amount of the carbon in the calcified tissue (Borowitzka, 1977).

4.2 δ^{13}C records

Average δ^{13}C values in AM-KR-80 were significantly lower than in Attu 11-4 (Fig. 5a).
Although a specimen-specific effect cannot be ruled out, we hypothesize that the lower
δ^{13}C values more likely result from the lower light levels to which the deeper AM-KR-80

(25 m) plant was exposed resulting in decreased photosynthesis relative to Attu 11-4 and AM4-1 (10 m) plants. Light levels are known to influence growth rates in coralline algae (Adey, 1970) and presumably photosynthesis as well. Decreased photosynthesis from lower light levels will reduce discrimination against δ^{13}C during growth, resulting in decreased δ^{13}C values in the skeleton. Therefore, the collection depth of an algal specimen (or more specifically, a factor that accounts for differences in ambient light regimes) needs to be taken into consideration before comparing δ^{13}C values among different specimens. In addition, since light levels may vary widely over very small spatial scales, for example as a result of local shading by macroalgae, averaging of more than one sample is recommended to reduce any influence of light on δ^{13}C values.

δ^{13}C values in marine calcium carbonate organisms are driven by changes in the $\delta^{13}C_{DIC}$, as well as any metabolic and kinetic effects that are present (e.g., McConnaughey, 2003). We hypothesize that kinetic effects are not a significant factor here (see Sect. 4.1), and assuming that offsets resulting from metabolic effects are constant over time and/or are accounted for by averaging multiple specimens, then δ^{13}C values largely reflect $\delta^{13}C_{DIC}$. Thus, the skeletal δ^{13}C records can reconstruct the primary factors influencing oceanic $\delta^{13}C_{DIC}$: anthropogenic δ^{13}C-Suess effect (Andreasson and Schmitz, 1998), surface-ocean primary production (Krantz et al., 1987), upwelling events (Killingley and Berger, 1979), and water column stratification (Arthur et al., 1983).

4.3 Secular decrease in δ^{13}C values

The decline in δ^{13}C values recorded by the coralline algal specimens examined in this study clearly exceeds what can be attributed to the δ^{13}C-Suess effect alone (Fig. 6). This enhanced rate of decline is not consistent with instrumental or proxy records from outside of the northern North Pacific Ocean and Bering Sea (e.g., Swart et al., 2010). This indicates that factors in addition to the δ^{13}C-Suess effect drive the skeletal δ^{13}C values. δ^{13}C values in bowhead whale baleen and steller sea lions bone collagen (Schell, 2000, 2001; Hirons et al., 2001) also decline at an enhanced rate; therefore,

an algal-specific effect or site-specific variability are unlikely to be the primary cause of the decline observed in our study. It would appear more likely that changes in the $\delta^{13}C_{DIC}$ pool to which both coralline algae and phytoplankton are exposed (the latter subsequently transmitted via the food web to whales and sea lions) drive the strongly
5 decreasing $\delta^{13}C$ values. Therefore, we explore the factors that influence $\delta^{13}C_{DIC}$, in addition to the $\delta^{13}C$-Suess effect, that may drive the enhanced rate of decline.

$\delta^{13}C_{DIC}$ in the northern North Pacific Ocean and Bering Sea regions is largely controlled by biological activity and upwelling/deep-water mixing (Tanaka et al., 2003). A decrease in primary productivity would increase the amount of CO_2 in surface waters,
10 thus reducing carbon fractionation during the calcification process and lead to lower $\delta^{13}C$ values in the resulting calcified tissues. In fact, a decline in phytoplankton cell growth rates, and hence primary productivity, has been hypothesized to drive the declining trends in the whale baleen and sea lion bone collagen $\delta^{13}C$ (Schell, 2000, 2001; Hirons et al., 2001). However, available evidence does not support a decrease in new
15 primary production (e.g., Hunt Jr. et al., 2002). In addition, there is no multi-year trend of decrease in growth-increment widths in the three *C. nereostratum* specimens over the past 50 years.

An increase in upwelling and/or deepening of the mixed layer would also change CO_2 concentrations in the surface waters of northern North Pacific Ocean and Bering Sea
20 (Patra et al., 2005), and thus $\delta^{13}C_{DIC}$ values and $\delta^{13}C$ values of the algal calcified tissues. Authors of previous reports have suggested that upwelling and deep mixing may reduce the influence of the Suess effect in the subarctic Pacific as a consequence of dilution by deep water that has not been influenced by anthropogenic carbon emissions and the limited amount of time for CO_2 equilibration to take place (Gruber et al., 1999;
25 Quay et al., 1992; Schell, 2001; Sonnerup et al., 1999). However, CO_2 concentrations increase and $\delta^{13}C_{DIC}$ decreases with depth (e.g, Koopnick et al., 1972; $\delta^{13}C_{DIC}$ decrease by up to ~2‰ within the top 200 m of the water column in measurements from WOCE_P13N, http://cdiac3.ornl.gov/waves/discrete), and the ability of upwelling and/or mixing of deep water to drive surface water $\delta^{13}C_{DIC}$ values has previously been

reported by Bacastow et al. (1996). Increased CO_2 concentrations resulting from more upwelling and/or deepening of the mixed layer theoretically decreases fractionation during calcification resulting in lower $\delta^{13}C$ values of the calcified tissue. In addition, the deeper water brought up to the surface will have low $\delta^{13}C_{DIC}$ values due to the
5 remineralization of organic matter with depth, thus contributing to decreased $\delta^{13}C_{DIC}$ in surface waters. The mixed layer depth in the subarctic North Pacific has shoaled in recent decades, which has been attributed to warming and freshening that in turn has produced enhanced stratification of the surface waters (Freeland et al., 1997); therefore, upwelling is likely the driving factor of the enhanced rate of decline in the
10 $\delta^{13}C$ proxy records. Changes in the Aleutian Low pressure system may be driving the increase in upwelling. When the low pressure system is intense, oceanic upwelling under the centre of the Aleutian Low is increased (Reid, 1962; Thomson, 1981), bringing higher concentrations of CO_2 with low $\delta^{13}C$ values to the surface. This upwelled CO_2 is moved to the edges of the Alaska gyre via horizontal divergence (similar to other
15 nutrients and biomass; Brodeur and Ware 1992; Reid 1962) and is incorporated into the Alaskan Stream. Once incorporated into the Alaskan Stream, the CO_2-rich water flows southwestward along the continental slope of the Alaska Peninsula and enters the Bering Sea through the Aleutian Island Archipelago. By this mechanism, CO_2-rich water was transported to the environment in which the algal specimens grew. In con-
20 trast, when the Aleutian Low weakens, oceanic upwelling is reduced and water with less CO_2 and lower $\delta^{13}C$ values is brought to the surface. The Aleutian Low Pressure Index (ALPI), which is a measure of the intensity of the Aleutian Low (Beamish et al., 1997), indicates that the Aleutian Low has generally been increasing in strength since the late-1940s (Fig. 6). In addition, the large scale variability in the ALPI is mirrored
25 with an approximately three-year lag in the algal $\delta^{13}C$ records from the start of the records up to 1989, which corresponds to the 1989 regime shift evident in the ALPI and in biological records (Beamish et al., 1999; Hare and Mantua, 2000). The lag likely represents the interval of time between the change in the pressure system, increase or decrease in upwelling, and transport of the water to the central Aleutian Islands where

the δ^{13}C ultimately is taken up by the algae. The cause of the decoupling between the Aleutian Low and the algal δ^{13}C records after the 1989 regime shift is unknown.

There is large spatial and temporal variability in upwelling and ocean currents, and consequently CO_2 concentrations, throughout the subarctic North Pacific (Stabeno et al., 2004; Murphy et al., 2001). Therefore, the location of a specific $\delta^{13}C_{DIC}$ record relative to upwelling and/or currents transporting the upwelled water explains the large variability in δ^{13}C instrumental and/or proxy records. The variable rate of decline recorded by the different instrumental and proxy records likely reflects local changes in $\delta^{13}C_{DIC}$ instead of basin-wide changes. As a consequence, extrapolation of a single record from one location to the entire basin provides an incomplete picture of carbon dynamics in the northern North Pacific Ocean and Bering Sea. Additional records are urgently needed to further constrain changes occurring and to calculate the role of subarctic oceans in taking up anthropogenic CO_2.

4.4 Detrended δ^{13}C variability

The significant spectral power on interannual timescales (4–7 years; Fig. 7) in the detrended and combined δ^{13}C record corresponds to fluctuations of the El Niño Southern Oscillation (ENSO). Authors of previous studies suggested an atmospheric link between the tropical ENSO events and the northern Pacific/Bering Sea related to the winter position of the Aleutian Low such that it is intense and shifts eastward during El Niño conditions, driving warm, moist air northward along the northeast Pacific coast towards Alaska and into the Bering Sea (Niebauer, 1988; Emery and Hamilton, 1985). The increase in intensity of the Aleutian Low associated with El Niño conditions will increase upwelling, bringing more CO_2-rich water with low δ^{13}C values into the surface waters. In contrast, a weakened Aleutian Low corresponds to cold events in the tropics (Emery and Hamilton, 1985). This supports a link between the tropical Pacific ENSO, and the subarctic Aleutian Low and algal δ^{13}C records driving the 4–7 year variability. The significant spectral power on approximately 16-year timescales (Fig. 7) is generally

consistent with the bidecadal (15–25 year) variations in the North Pacific Index (NPI) (Minobe, 1999). The NPI is another time series index representing the Aleutian Low, and is inversely correlated to the ALPI. Thus similar patterns between the NPI and the algal δ^{13}C values are expected. These relationships support the influence of shifts in climate regimes (i.e., ENSO, PDO) on the surface water δ^{13}C$_{DIC}$ values, in addition to the anthropogenic δ^{13}C-Suess effect.

5 Summary

δ^{13}C values from coralline algae clearly measure a decrease in δ^{13}C values over the past 30 years exceeding that due solely to the anthropogenic δ^{13}C-Suess effect. The enhanced rate of decline is consistent with records from some marine mammals. This indicates that the δ^{13}C$_{DIC}$ which is taken up by primary producers, i.e., phytoplankton at the bottom of the marine food web and benthic coralline algae, is the cause of the enhanced rate of decline. We hypothesize that a combination of the δ^{13}C-Suess effect and an increasingly intense Aleutian Low drives the strongly decreasing δ^{13}C values. An intense Aleutian Low increases upwelling of CO_2-rich water to the surface with a low δ^{13}C signature. The higher concentrations of CO_2 in the surface water will decrease fractionation by the algae during photosynthesis, lowering δ^{13}C values of the calcified tissue. The combined and detrended dataset varies on ENSO and bidecadal scales supporting an atmospheric teleconnection between the tropics and the subarctic Pacific. This study demonstrates the utility of coralline algal δ^{13}C records in understanding the factors influencing δ^{13}C$_{DIC}$, and cautions that spatially-limited records should not be extrapolated to describe carbon dynamics for the entire northern Pacific Ocean and Bering Sea.

References

Adey, W.: The effects of light and temperature on growth rates in boreal-subarctic crustose corallines, J. Phycol., 6, 269–276, 1970.

Andreasson, F. and Schmitz, B.: Tropical Atlantic seasonal dynamics in the Early Middle Eocene from stable oxygen and carbon isotope profiles of mollusk shells, Paleoceanography, 13, 183–192, doi:110.1029/1098PA00120, 1998.

Arthur, M., Williams, D., and Jones, D.: Seasonal temperature-salinity changes and thermocline development in the mid-Atlantic Bight as recorded by the isotopic composition of bivalves, Geology, 11, 655–659, 1983.

Bacastow, R., Keeling, C., Lueker, T., Wahlen, M., and Mook, W.: The ^{13}C Suess Effect in the World Surface Oceans and Its Implications for Oceanic Uptake of CO_2: Analysis of Observations at Bermuda, Global Biogeochem. Cy., 10, 335–346, 1996.

Beamish, R., Neville, C., and Cass, A.: Production of Fraser River sockeye salmon (Oncorhynchus nerka) in relation to decadal-scale changes in the climate and the ocean, Can. J. Fish. Aquat. Sci., 54, 543–554, 1997.

Beamish, R., Noakes, D., McFarlane, G., Klyashtorin, L., Ivanoc, V., and Kurashov, V.: the regime concept and natural trends in the production of Pacific salmon, Can. J. Fish. Aquat. Sci., 56, 516–526, 1999.

Benson, A. and Trites, A.: Ecological effects of regime shifts in the Bering Sea and eastern North Pacific Ocean, Fish Fish., 3, 95–113, 2002.

Borowitzka, M.: Algal calcification, Oceanography and Marine Biology, an Annual Review, 15, 189–223, 1977.

Brodeur, R. and Ware, D.: Long-term variability in zooplankton biomass in the subarctic Pacific Ocean, Fish. Oceanogr., 1, 32–38, 1992.

Cooper, L., Whitledge, T., Grebmeier, J., and Weingartner, T.: The nutrient, salinity and stable oxygen isotope composition of Bering and Chukchi Seas waters in and near the Bering Strait, J. Geophys. Res., 102, 12563–512573, 1997.

Emery, W. and Hamilton, K.: Atmospheric forcing of interannual variability in the Northeast Pacific Ocean: connections with El Niño, J. Geophys. Res., 90, 857–868, 1985.

Freeland, H., Denman, K., Wong, C., Whitney, F., and Jacques, R.: Evidence of change in the winter mixed layer in the Northest Pacific Ocean, Deep-Sea Res. Pt. I, 44, 2117–2129, 1997.

Gruber, N., Keeling, C. D., Bacastow, R. B., Guenther, P. R., Lueker, T. J., Wahlen, M., Meijer, H. A. J., Mook, W. G., and Stocker, T. F.: Spatiotemporal patterns of carbon-13 in the global surface oceans and the oceanic Suess effect, Global Biogeochem. Cy., 13, 307–335, 1999.

Halfar, J., Zack, T., Kronz, A., and Zachos, J.: Growth and high-resolution paleoenvironmental signals of rhodoliths (coralline red algae): a new biogenic archive, J. Geophys. Res., 105, 22107–122116, 2000.

Halfar, J., Steneck, R., Schone, B., Moore, G., Joachimski, M., Kronz, A., Fietzke, J., and Estes, J.: Coralline alga reveals first marine record of subarctic North Pacific climate change, Geophys. Res. Lett., 34, L07702, doi:07710.01029/02006GL028811, 2007.

Halfar, J., Steneck, R., Joachimski, M., Kronz, A., and Wanamaker Jr., A.: Coralline red algae as high-resolution climate recorders, Geology, 36, 463–466, 2008.

Hare, S. and Mantua, N.: Empirical evidence for North Pacific regime shifts in 1977 and 1989, Prog. Oceanogr., 47, 103–145, 2000.

Hetzinger, S., Halfar, J., Kronz, A., Steneck, R., Adey, W., Lebednik, P., and Schone, B.: High-resolution Mg/Ca ratios in a coralline red alga as a proxy for Bering Sea temperature variations from 1902 to 1967, Palaios, 24, 406–412, doi:410.2110/palo.2008.p2108-2116r, 2009.

Hirons, A., Schell, D., and Finney, B.: Temporal records of d^{13}C and d^{15}N in North Pacific pinnipeds: inferences regarding environmental change and diet, Oecologia, 129, 591–601, 2001.

Hobson, K., Sinclair, E., Yorkz, A., Tomason, J., and Merrick, R.: Retrospective isotopic analyses of Stellar sea lion tooth annuli and sea-bird feathers: a cross-taxa approach to investigating regime and dietary shifts in the Gulf of Alaska, Marine Mammal Science, 20, 621–638, 2004.

Hunt Jr., G., Stabeno, P., Walters, G., Sinclair, E., Brodeur, R., Napp, J., and Bond, N.: Climate change and control on the southeastern Bering Sea pelagic ecosystem, Deep-Sea Res. Pt. I, 49, 5821–5853, 2002.

Jimenez-Lopez, C., Romanek, C., and Caballero, E.: Carbon isotope fractionation in synthetic magnesian calcite, Geochim. Cosmochim. Ac., 70, 1163–1171, 2006.

Kamenos, N., Cusack, M., Huthwelker, T., Lagarde, P., and Scheibling, R.: Mg-lattice associations in red coralline algae, Geochim. Cosmochim. Ac., 73, 1901–1907, 2009.

Keeling, C. D., Piper, S. C., Bacastow, R. B, Wahlen, M., Whorf, T. P., Heimann, M., et al.: Exchanges of Atmospheric CO_2 and $^{13}CO_2$ with the Terrestrial Biosphere and Oceans from 1978 to 2000, I., Global Aspects, UC San Diego, Scripps Institution of Oceanography, 2001.

Key, R., Kozyr, A., Sabine, C., Lee, K., Wanninkhof, R., Bullister, J., Feely, R., Millero, F., Mordy, C., and Peng, T.-H.: A global ocean carbon climatology: Results from Global Data Analysis Project (GLODAP), Global Biogeochem. Cy., 18, GB4031, doi:4010.1029/2004GB002247, 2004.

Killingley, J. and Berger, W.: Stable Isotopes in a Mollusk Shell: detection of Upwelling Events, Science, 205, 186–188, doi:110.1126/science.1205.4402.1186, 1979.

Kim, S.-T. and O'Neil, J.: Equilibrium and nonequilibrium oxygen isotope effects in synthetic carbonates, Geochim. Cosmochim. Ac., 61, 3461–3475, 1997.

Krantz, D., Williams, D., and Jones, D.: Ecological and paleoenvironmental information using stable isotope profiles from living and fossil molluscs Palaeogeogr. Palaeocl., 58, 249–266, doi:210.1016/0031-0182(1087)90064-90062, 1987.

Kroopnick, P., Weiss, R., and Craig, H.: Total CO_2,^{13}C, and dissolved oxygen – ^{18}O at Geosecs II in the North Atlantic, Earth Planet. Sc. Lett., 16, 103–110, doi:110.1016/0012-1821X(1072)90242-90247, 1972.

Lebednik, P.: The corallinacea of northwestern North America, I, Clathromorphum Foslie emend. Adey, Syesis, 9, 59–112, 1976.

Lee, D. and Carpenter, S.: Isotoptic disequilibrium in marine calcareous algae, Chem. Geol., 172, 307–329, 2001.

McConnaughey, T.: Sub-equilibrium oxygen-18 and carbon-13 levels in biological carbonates: carbonate and kinetic models, Coral Reefs, 22, 316–327, 2003.

McFarlane, G. A., King, J. R., and Beamish, R. J.: Have there been recent changes in climate?, Ask the fish., Prog. Oceanogr., 47, 147–169, 2000.

Minobe, S.: Resonance in bidecadal and pentadecadal climate oscillations over the North

Pacific: role in climatic regime shifts, Geophys. Res. Lett., 26, 855–858, 1999.

Münchow, A., Weingartner, T., and Cooper, L.: The summer hydrography and surface circulation of the East Siberian Shelf Sea, J. Phys. Oceanogr., 29, 2167–2182, 1999.

Murphy, P., Nojiri, Y., Harrison, D., and Larkin, N.: Scales of spatial variability for surface ocean pCO$_2$ in the Gulf of Alaska and Bering Sea: Toward a sampling strategy, Geophys. Res. Lett., 28, 1047–1050, doi:1010.1029/2000GL012375, 2001.

Newsome, S., Etnier, M., Kurle, C., Waldbauer, J., Chamberlain, C., and Koch, P.: Historic decline in primary productivity in western Gulf of Alaska and eastern Bering Sea: isotopic analysis of northern fur seal teeth, Marine Ecology Progress Series, 332, 211–224, 2007.

Niebauer, H.: Effects of El Nino-Southern Oscillation and North Pacific weather patterns on interannual variability in the subarctic Bering Sea, J. Geophys. Res., 93, 5051–5068, doi:10.1029/JC1093iC1005p05051, 1988.

Paillard, D., Labeyrie, L., and Yiou, P.: Macintosh program performs timeseries analysis, EOS, Transactions, American Geophysical Union, 77, 379, 1996.

Patra, P., Maksyutov, S., Ishizawa, M., Nakazawa, T., Takahashi, T., and Ukita, J.: Interannual and decadal changes in the sea-air CO$_2$ flux from atmospheric CO$_2$ inverse modeling, Global Biogeochemi. Cy., 19, GB4013, doi:4010.1029/2004GB002257, 2005.

Quay, P., Tilbrook, B., and Wong, C.: Oceanic Uptake of Fossil Fuel CO$_2$: Carbon-13 Evidence Science, 256, 74–79, 1992.

Quay, P., Sonnerup, R., Westby, T., Stutsman, J., and McNichol, A.: Changes in the ^{13}C/^{12}C of dissolved inorganic carbon in the ocean as a tracer of anthropogenic CO$_2$ uptake, Global Biogeochem. Cy., 17, 1004, doi:1010.1029/2001GB001817, 2003.

Reed, R. and Stabeno, P.: Flow along and across the Aleutian Ridge, J. Mar. Res., 52, 639–648, 1994.

Reid, J.: On circulation, phosphate-phosphorus content, and zooplankton volumes in the upper part of the Pacific Ocean, Limnol. Oceanogr., 7, 287–306, 1962.

Romanek, C., Grossman, E., and Morse, J.: Carbon isotopic fractionation in synthetic aragonite and calcite: Effects of temperature and precipitation rate, Geochim. Cosmochim. Ac., 56, 419–430, 1992.

Sabine, C., Feely, R., Gruber, N., Key, R., Lee, K., Bullister, J., Wanninkhof, R., Wong, C., Wallace, D., Tilbrook, B., Millero, F., Peng, T.-H., Kozyr, A., Ono, T., and Rios, A.: The Oceanic Sink for Anthropogenic CO$_2$, Science, 305, 367–371, doi:310.1126/science.1097403, 2004a.

Sabine, C., Feely, R., Watanabe, Y., and Lamb, M.: Temporal Evolution of the North Pacific CO_2 Uptake Rate, J. Oceanogr., 60, 5–15, doi:10.1023/B:JOCE.0000038315.0000023875.ae, 2004b.

Schell, D.: Declining carrying capacity in the Bering Sea: isotopic evidence from whale baleen, Limnol. Oceanogr., 45, 459–462, 2000.

Schell, D.: Carbon isotope ratio variations in Bering Sea biota: the role of anthropogenic carbon dioxide, Limnol. Oceanogr., 46, 999–1000, 2001.

Schmidt, G., Bigg, G., and Rohling, E.: Global Seawater Oxygen-18 Database, http://data.giss. nasa.gov/o18data/, 1999.

Sonnerup, R., Quay, P., McNichol, A., Bullister, J., Westby, T., and Anderson, H.: Reconstructing the Oceanic 13C Suess Effect, Global Biogeochem. Cy., 13, 857–872, 1999.

Stabeno, P., Bond, N., Hermann, A., Kachel, C., Mordy, C., and Overland, J.: Meteorology and Oceanography of the Northern Gulf of Alaska, Cont. Shelf Res., 24, 859–897, 2004.

Swart, P.: Carbon and oxygen isotope fractionation in scleractinian corals: a review, Earth Sci. Rev., 19, 51–80, 1983.

Swart, P., Greer, L., Rosenheim, B., Moses, C., Waite, A., Winter, A., Dodge, R., and Helmle, K.: The ^{13}C Suess effect in scleractinian corals mirror changes in the anthropogenic CO_2 inventory of the surface oceans, Geophys. Res. Lett., 37, L05604, doi:05610.01029/02009GL041397, 2010.

Tanaka, T., Watanabe, Y., Watanabe, S., Noriki, S., Tsurushima, N., and Nojiri, Y.: Oceanic Suess effect of d^{13}C in subpolar region: The North Pacific, Geophys. Res. Lett., 30, 2159, doi:10.1029/2003GL018503, 2003.

Thomson, R.: Oceanography of the British Columbia Coast, Canadian Special Publication of Fisheries and Aquatic Sciences, National Research Council, Ottawa, 291 pp., 1981.

Torrence, C. and Compo, G.: A Practical Guide to Wavelet Analysis, B. Am. Meteorol. Soc., 79, 61–78, 1998.

Wefer, G. and Berger, W.: Isotope paleontology: growth and composition of extant calcareous species, Mar. Geol., 100, 207–248, 1991.

Williams, B., Risk, M., Stone, R., Sinclair, D., and Ghaleb, B.: Oceanographic changes in the North Pacific Ocean over the past century recorded in deep-water gorgonian corals, Marine Ecology Progress Series, 335, 85–94, 2007.

Title Page

Abstract | Introduction

Conclusions | References

Tables | Figures

◄ | ►

◄ | ►

Back | Close

Full Screen / Esc

Printer-friendly Version
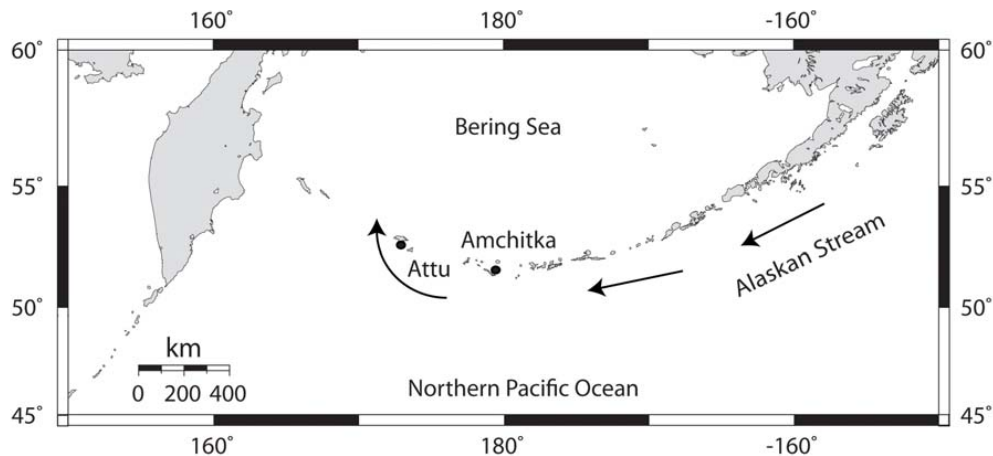
Interactive Discussion

Fig. 1. Location of sample collection sites offshore of Attu and Amchitka Islands along the Aleutian Arc in the northern North Pacific Ocean and Bering Sea. Black circle indicates sample locations. (Map generated at http://www.planiglobe.com.)
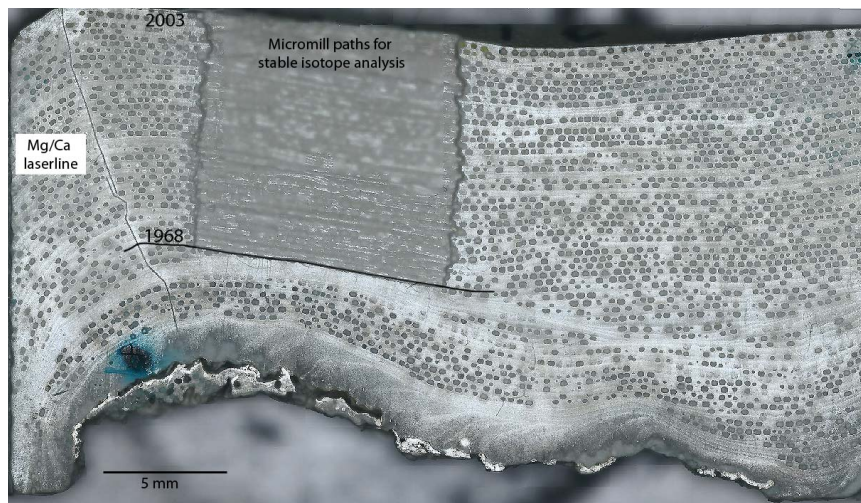
Full Screen / Esc

Fig. 2. Geo.ts photograph of polished section of specimen AM4-1 with laser transect and micromill path. Micromilling path ran parallel to growth increments. Clear annual growth increments from 2003 to 1968 were used in conjunction with Mg/Ca measured by laser ablation inductively coupled plasma mass spectrometry to develop a robust growth chronology for this specimen. Samples for stable isotope analysis were micromilled directly adjacent to the laser transects.
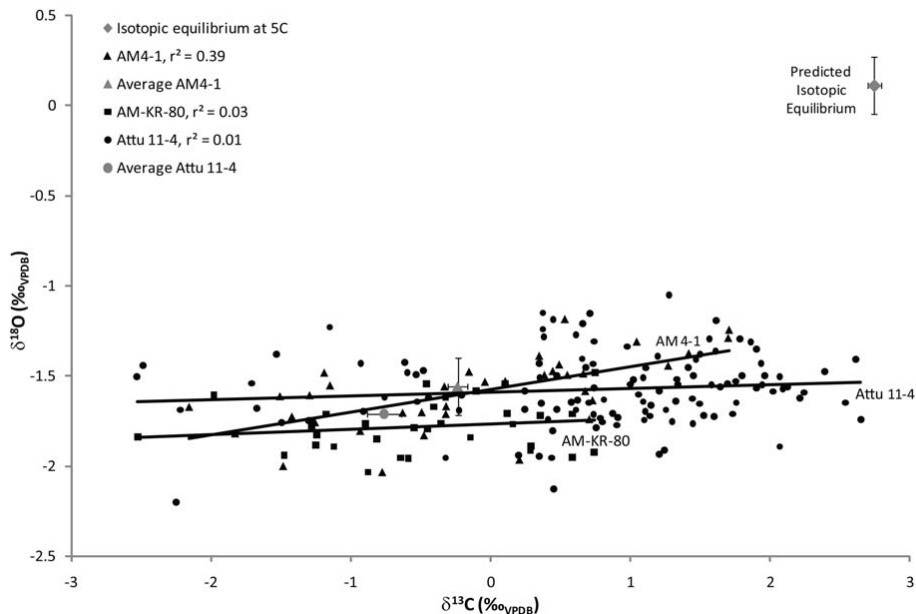
Fig. 3. δ^{18}O values plotted against δ^{13}C values for the calcified tissue of three specimens of coralline algae with regression lines. Larger grey symbols represent the average δ^{13}C (for 1992–1993) and δ^{18}O (for 1990, 1993, and 1995) for Attu11-4 and AM4-1. Predicted isotopic equilibrium for inorganic calcite is plotted (grey diamond) based on δ^{13}C and δ^{18}O values for seawater from 1992–1993 and 1990, 1993, and 1995, respectively, and equations from Romanek et al. (1992) and Kim and O'Neil (1997), respectively. The equation for δ^{18}O incorporated the addition of 0.17‰ for each mol % Mg according to Jiménez-López et al. (2006). 9.9 mol % Mg used was the median value from the range given in Hetzinger et al. (2009). Error bars indicate one standard error around the average. Error bars not visible are smaller than symbol. Predicted equilibrium is not plotted for AM-KR-80 as this sample was collected prior to the early 1990s.
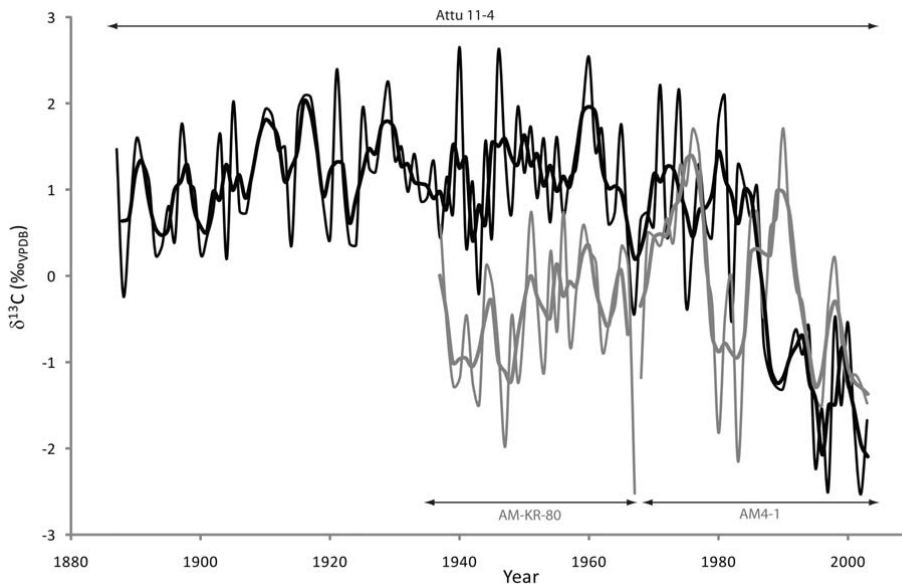
Printer-friendly Version

Interactive Discussion

Fig. 4. Annually-resolved δ^{13}C values for three *Clathromorphum nereostratum* specimens collected offshore of the Aleutian Islands with 3-year running mean in bold.
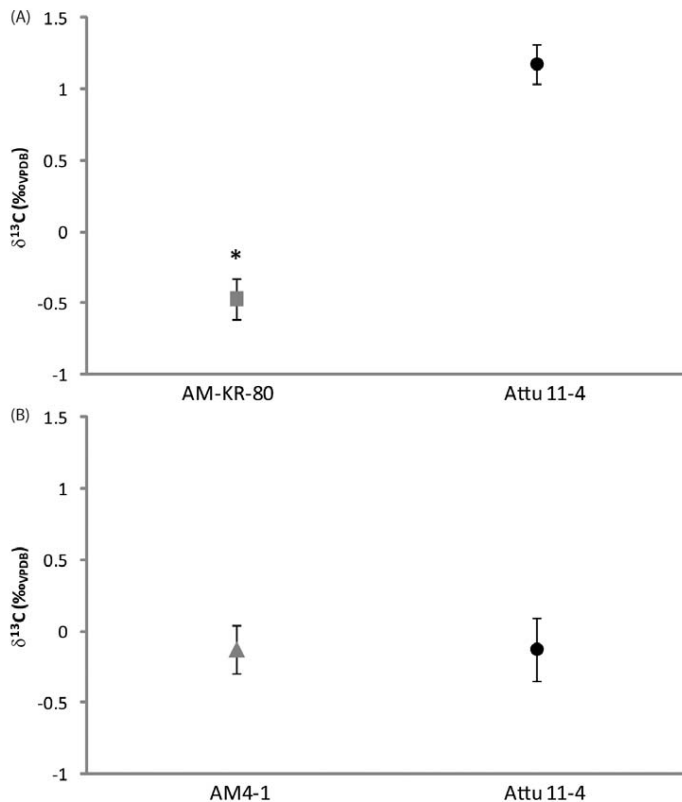
Fig. 5. Average (± SE) δ^{13}C values for **(A)** AM-KR-80 and Attu 11-4 for the common period of 1937–1967 and **(B)** for AM4-1 and Attu 11-4 for the common period of 1968–2003. Averages were calculated from annual values as described in the methods section. * indicates significant differences between averages according to a t-test.
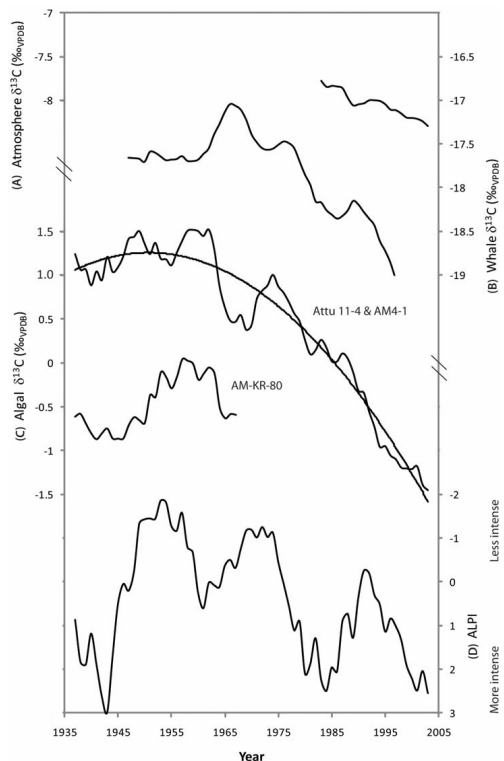
Fig. 6. **(A)** Annual atmospheric $\delta^{13}C$ values from Pt. Barrow, Alaska (data from Keeling et al. (2001); http://scrippsco2.ucsd.edu/data/flask_co2_and_isotopic/monthly_iso/monthly_ptb_c13.csv), **(B)** $\delta^{13}C$ values from the baleen of bowhead whales (data from Schell et al., 2001), **(C)** $\delta^{13}C$ values from algal specimen AM-KR-80 and combined $\delta^{13}C$ values from specimens Attu 11-4 (1937–1967) and AM4-1 and Attu 11-4 (1968–2003) with line of best fit calculated using SigmaPlot (Systat Software Inc., San Jose, CA), and **(D)** ALPI values (data from Beamish et al., 1997; http://www.pac.dfo-mpo.gc.ca/science/species-especes/climatology-ie/cori-irco/indices/alpi.txt). Whale, algal and ALPI datasets were smoothed with a 7-year running mean. Algal and whale $\delta^{13}C$ values decrease at a rate exceeding that expected due solely to the $\delta^{13}C$-Suess effect and likely reflects the combined influence of the $\delta^{13}C$-Suess effect and an intensifying ALPI. Note that the y-axis for the ALPI is reversed.

Title Page

Abstract | Introduction

Conclusions | References

Tables | Figures

|◄ | ►|

◄ | ►

Back | Close

Full Screen / Esc

Printer-friendly Version

Interactive Discussion

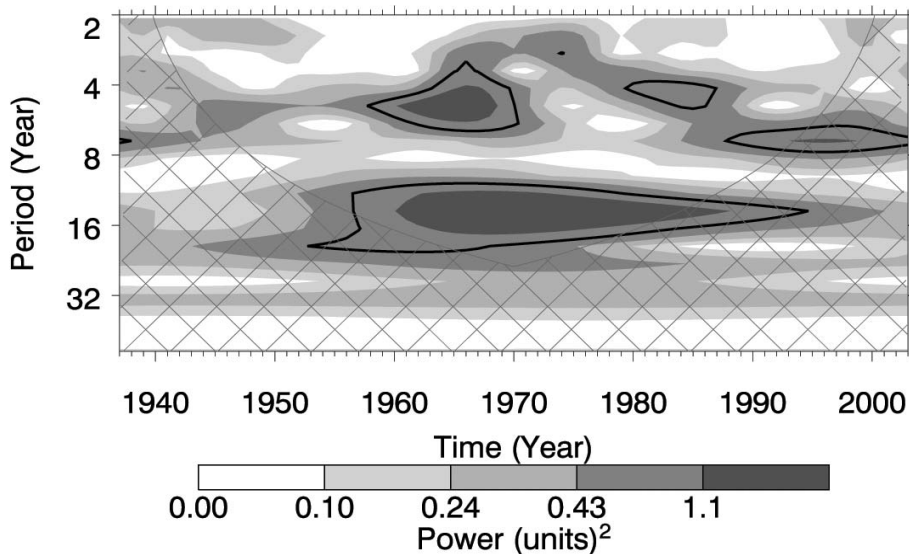**Fig. 7.** The wavelet power spectrum for δ^{13}C values from detrended and combined dataset from 1937 to 2003. The contour levels are chosen so that 75%, 50%, 25%, and 5% of the wavelet power is above each level, respectively. The cross-hatched region is the cone of influence, where zero padding has reduced the variance. Black contour is the 10% significance level, using a white-noise (autoregressive lag1) background spectrum. Analyses made using IDL Wavelet Toolkit (Torrence and Compo 1998; available at: http://paos.colorado.edu/research/wavelets/).